

Supporting Info for

Orientational Distribution of DPH in Lipid Membranes: a Comparison of Molecular Dynamics Calculations and Experimental Time-Resolved Anisotropy Experiments

Markéta Paloncýová^{1,2}, Marcel Ameloot,² Stefan Knippenberg*^{1,2}

¹ Department of Theoretical Chemistry and Biology, KTH Royal Institute of Technology, Stockholm, Sweden

² Biomedical Research Institute, Hasselt University, Agoralaan Building C, 3590 Diepenbeek, Belgium

* Author to which correspondence should be sent: stefan.knippenberg@uhasselt.be

Table of contents

Figure S1: Time evolution of the distance of the DPH center of mass to the middle of the membrane	2
Figure S2: Time evolution of the orientation of the transition dipole moment with respect to the z-axis	3
Table S1: Average time of rotation, permeations and flip flops and respective residence lifetimes	4
Figure S3: Orientation of the transition dipole moment to the z-axis when the probe is located in the membrane center	4
Figure S4: Autocorrelation function $\langle \sin^2 \Delta\varphi \rangle$	5
Table S2: Fluorescence anisotropy data	6
Figure S5: Comparison of the orientation distributions of DPH monitored in MD simulations and recalculated by maximum entropy model	7
Figure S6: fraction of parallel, tilted and perpendicular orientation as monitored in MD simulations and recalculated from the θ distribution	7
Table S3: the experimental data and the θ distributions calculated from $\langle P_2 \rangle$ and $\langle P_4 \rangle$, with and without rescaling	8
Figure S7: convergences of the MD calculations based on the various anisotropy decay curves	9
Discussion about the local environment of the DPH fluorophore which can be probed through deuterium order parameters	10
Figure S8: Correlation of the limiting value of ROTACF (C_∞) with the deuterium order parameters $\langle S_{CD} \rangle$	10

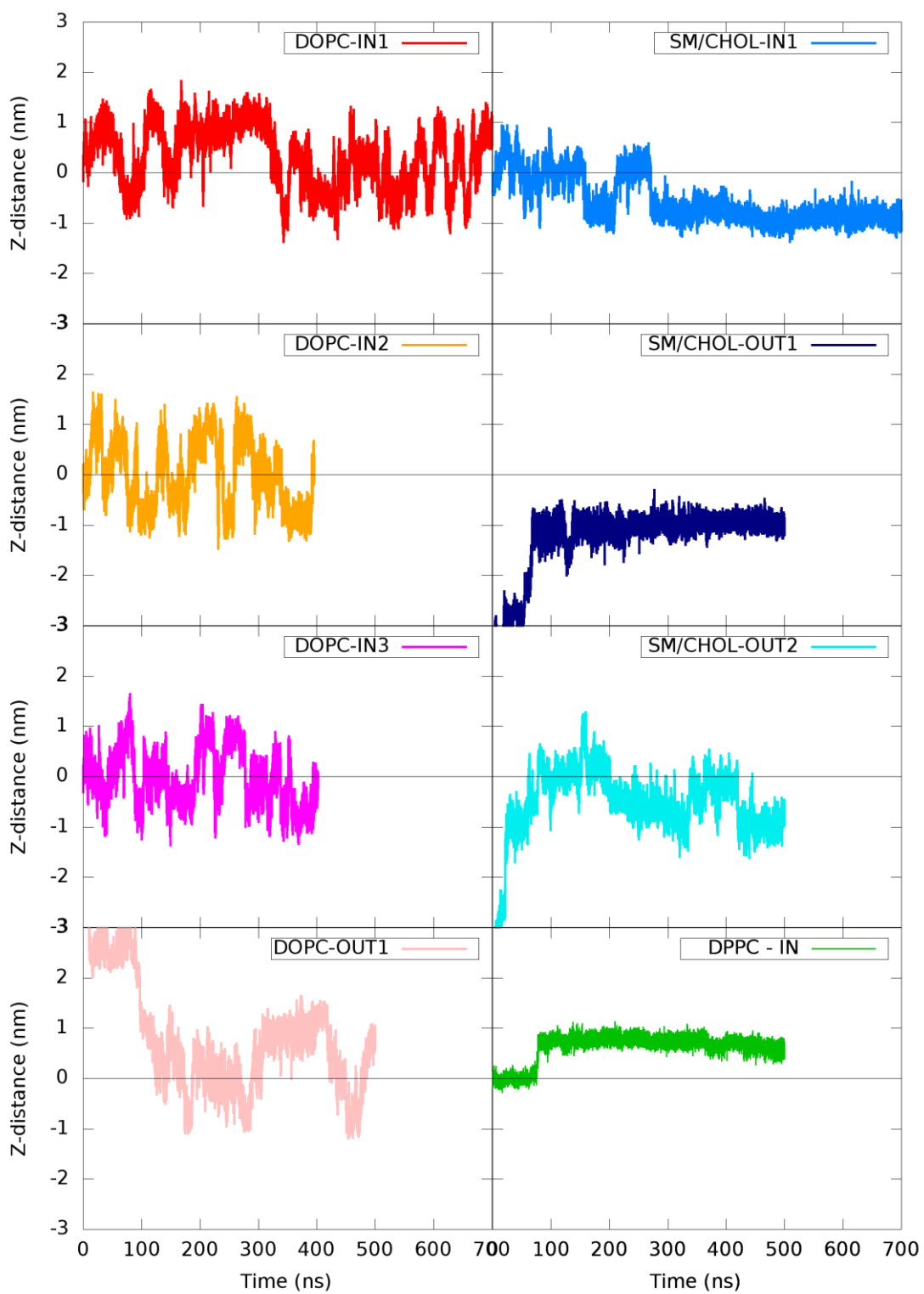


Figure S1: Time evolution of the distance of DPH centre of mass to the middle of the membrane.

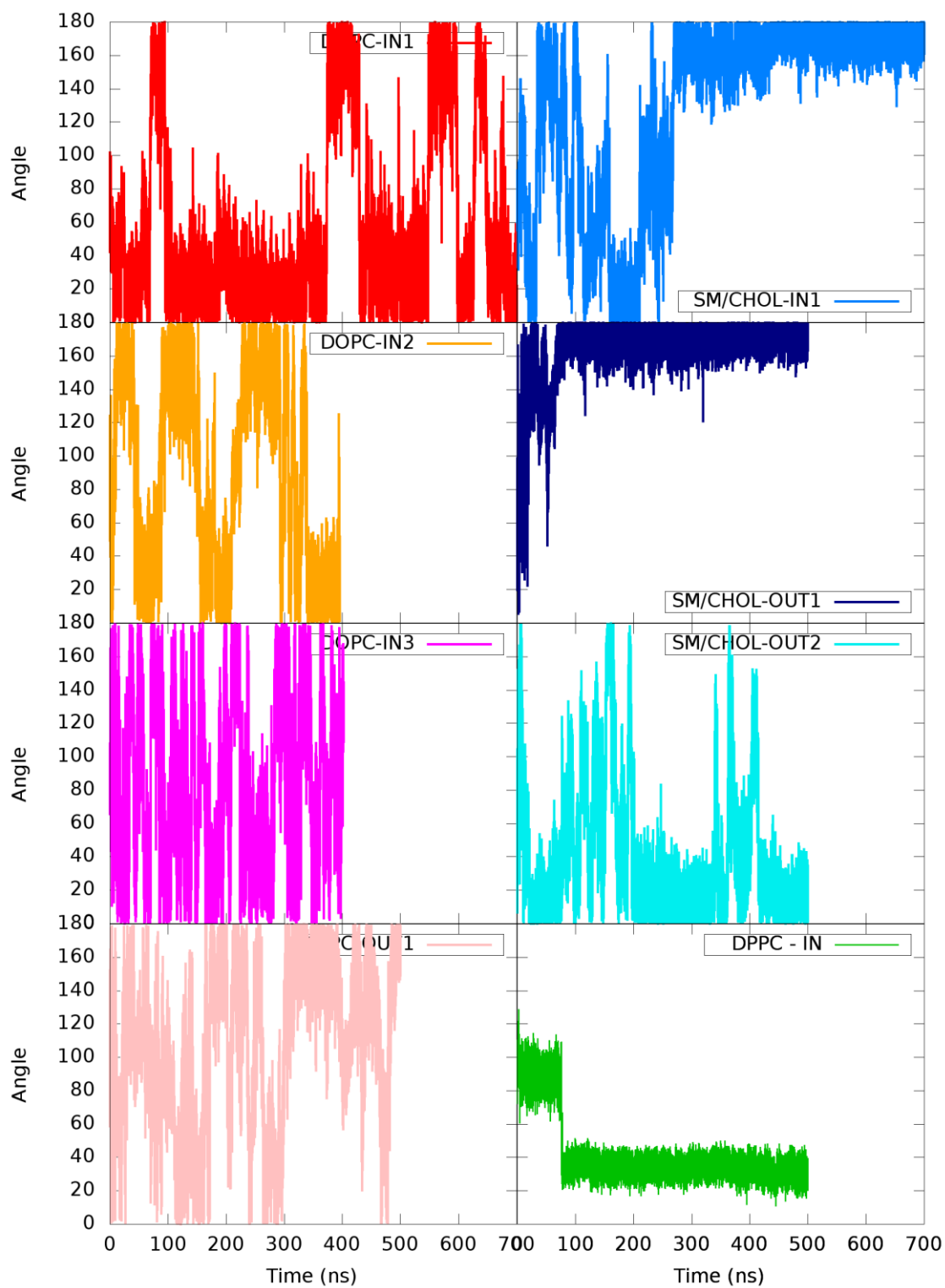


Figure S2: Time evolution of the orientation of the transition dipole moment with respect to the z-axis (right).

Table S1: Average time between observed half or full rotations of DPH within 100 ns of MD simulations, (in terms of angle of DPH transition dipole moment (TDM) with respect to the z-axis, θ ; half – 0-90° or 90-180° or vice versa; full – 0-180°), number (#) of observed events and time in ns spent in flat orientation (parallel to membrane surface) or tail orientation (TDM parallel to lipid tails) in individual systems.

Average time between observed half or full DPH permeation (in terms of distance of the centre of mass of DPH to the membrane middle; half: 0.0 to ± 0.95 nm or back; full: -0.95 to +0.95 nm or back), and time spent in membrane middle or in membrane tails.

Average time in ns spent in between the leaflets of the membrane in ‘flat’ orientation and average time spent in membrane tails in ‘tails’ orientation during flip-flopping. Analysed simulation time (after 200 ns equilibration period) is given in the last column. Full description of analysis and the regions’ borders can be found in Methods section.

		Rotation						Permeation						Flip-flop		A
		Half		Full		Flat	Tails	Half		Full		Middle	Tails	Flat - middle	Tails	
		ns	#	ns	#	ns		ns	#	ns	#	ns		ns		ns
DOPC	IN1	9.4	52	75	6	1.6	12.6	16.1	30	58.2	8	17.7	15.3	2.5	15.5	500
	IN3 ^a	6.3	30	17.4	8	2.9	9.5	13	14	18.8	5	8.8	15	2.3	19.9	195
	IN4 ^a	1.7	118	9.1	22	1.3	2.1	10.1	19	25.8	3	8.7	12.1	2.3	4.1	201
	OUT1	5.9	50	47.1	6	3.8	8.1	12.4	23	69.2	4	10.5	14.3	3.4	10.8	300
SM/C HOL	IN1	45.5	10	23.2	3	10.6	87.3	166.7	2		0	62.4	424.8	13.4	422.7	500
	OUT1	300	0		0			300	0		0					300
	OUT2 ^a	23.1	12	88.8	2	6.1	43.8	18.7	15		0	14.1	20	6.5	22.6	300
DPPC - IN			0		0		300+		0		0		300+		300+	300

^a Extra simulations for the probe initially out- and inside the membrane have been performed to enable a discussion about convergence issues in anisotropy calculations – see Figure S7 and related text there.

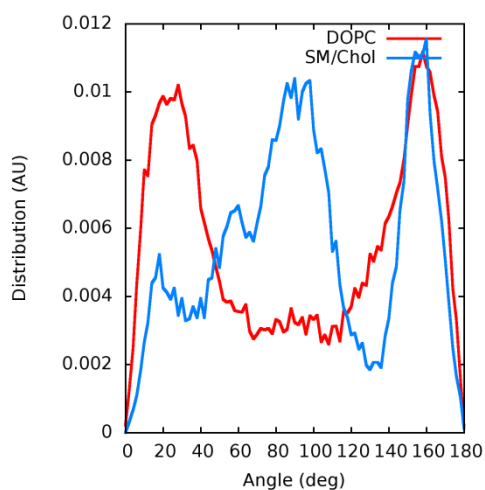


Figure S3: Orientation of the transition dipole moment to the z-axis when the probe is located in the membrane center (position of DPH center of mass within 0.1 nm from the center of the membrane in the z-direction). For each system, all simulations are merged for the analysis.

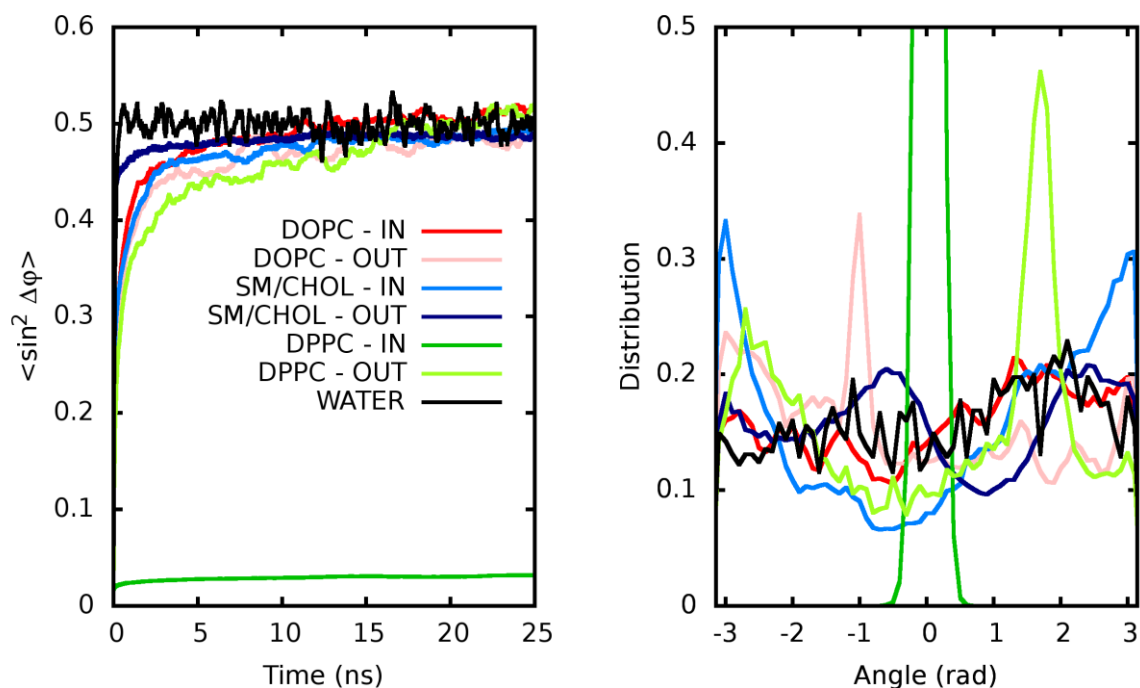


Figure S4: Autocorrelation function $\langle \sin^2 \Delta\phi \rangle$ converges to 0.5 (left), showing a random distribution of DPH transition dipole moment in azimuthal direction (right). In DPPC – IN simulation the DPH adopted just one orientation and did not sample the whole azimuthal space.

Table S2: Fluorescence anisotropy data calculated through our MD simulations (Eq. 4) fitted to the Wobbling in a Cone (Eq. 6) and General model (Eq. 8) with extracted order parameters $\langle P_2 \rangle$ and $\langle P_4 \rangle$, relaxation time for the cone model (t_1), rotational diffusion coefficient (D) and limiting anisotropies (C_∞). The cone angles θ_c were calculated based on Eq. 7 from C_∞ . Further, raw MD simulations are analysed in order to calculate $\langle P_2 \rangle$ and $\langle P_4 \rangle$ and D . The analysis of the angle TDM of DPH to the membrane normal (θ) distribution is provided in terms of fraction parallel ($\theta < 30^\circ$), tilted ($30^\circ < \theta < 60^\circ$) and perpendicular ($\theta > 60^\circ$). Fractions are calculated from the raw MD data (MD), recalculated from the distribution defined by $\langle P_2 \rangle$ and $\langle P_4 \rangle$ from the raw MD data (θ), from the distribution calculated by the general Rg3 model (Rg3) and from the Rg3 model with adjusted $\langle P_4 \rangle$ (Rg3-adj).

		DOPC				SM/CHOL			DPPC	
		IN	OUT	IN ^{2a}	IN ^{3a}	IN	OUT	OUT ^{2a}	IN	OUT ^b
Wobbling in a cone (Eq. 6)	t_1	1.17	1.63	1.44	0.63	1.41	0.23	1.60	0.25	1.14
	C_∞	0.38	0.19	0.26	0.13	0.73	0.93	0.56	0.97	0.08
	θ_c	44.4	56.1	50.9	61.0	25.8	13.0	34.9	7.9	65.9
	$\langle P_2 \rangle$	0.61	0.43	0.51	0.36	0.86	0.96	0.75	0.99	0.18
	$\langle P_4 \rangle$	0.09	-0.09	-0.03	-0.12	0.57	0.88	0.32	0.95	-0.13
$10^{\text{th}} \langle S_{\text{CD}} \rangle$		0.18	0.17	0.16	0.16	0.37	0.40	0.37	0.20	
General model (Eq. 8)	$\langle P_2 \rangle$	0.61	0.40	0.50	0.35	0.85	0.96	0.74	0.99	-0.14
	$\langle P_4 \rangle$	0.59	0.56	0.64	0.52	0.78	0.92	0.72	0.97	0.50
	D_\perp (ns ⁻¹)	0.24	0.29	0.44	0.75	0.09	0.13	0.18	0.05	1.01
Raw MD analysis (Eq. 9,10)	$\langle P_2 \rangle$	0.60	0.37	0.47	0.27	0.77	0.96	0.70	0.53	-0.10
	$\langle P_4 \rangle$	0.26	0.14	0.20	0.04	0.65	0.86	0.46	-0.12	0.09
	D_\perp (ns ⁻¹)	0.51	0.56	0.59	0.91	0.39	0.28	0.52	0.14	3.25
Perpendicular Fraction	MD	0.07	0.22	0.17	0.26	0.09	0.00	0.07	0.00	0.62
	θ	0.07	0.23	0.16	0.26	0.09	0.00	0.08	0.00	0.62
	Rg3	0.20	0.36	0.30	0.38	0.06	0.01	0.13	0.00	0.70
	Rg3-adj	0.06	0.21	0.19	0.21	0.01	0.00	0.05	0.00	0.52
Parallel Fraction	MD	0.61	0.41	0.51	0.30	0.84	1.00	0.77	0.18	0.12
	θ	0.61	0.41	0.50	0.30	0.86	1.00	0.76	0.18	0.13
	Rg3	0.75	0.61	0.68	0.57	0.93	0.99	0.85	1.00	0.24
	Rg3-adj	0.60	0.45	0.58	0.37	0.92	1.00	0.80	1.00	0.17
Tilted Fraction	MD	0.33	0.36	0.32	0.44	0.07	0.00	0.16	0.82	0.25
	θ	0.32	0.36	0.33	0.43	0.05	0.00	0.16	0.82	0.26
	Rg3	0.05	0.04	0.02	0.05	0.01	0.00	0.02	0.00	0.06
	Rg3-adj	0.35	0.33	0.23	0.42	0.08	0.00	0.15	0.00	0.31

^a Extra simulations for the probe initially out- and inside the membrane has been performed to enable a discussion about convergence issues in anisotropy calculations – see Figure S7 and related text there.

^b Not entering the membrane

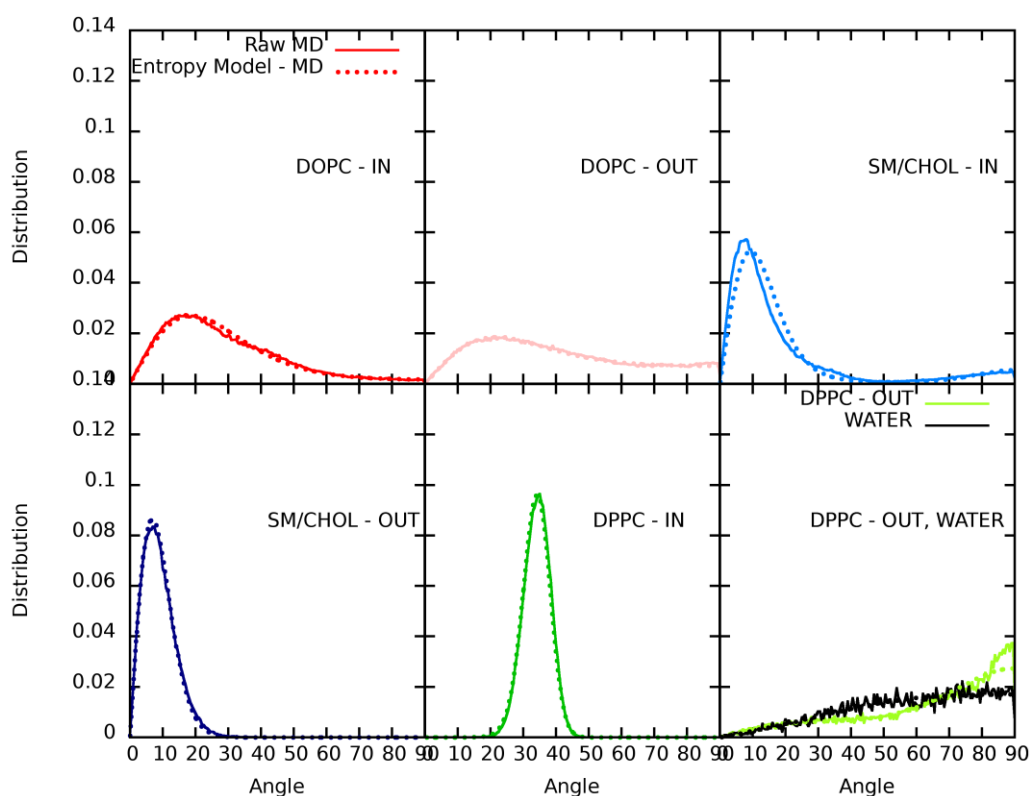


Figure S5: Distribution functions of the angle of the DPH transition dipole moment and the membrane normal monitored in MD simulations (solid line) and recalculated by the maximum entropy model (dotted line). The differences in the distributions are negligible.

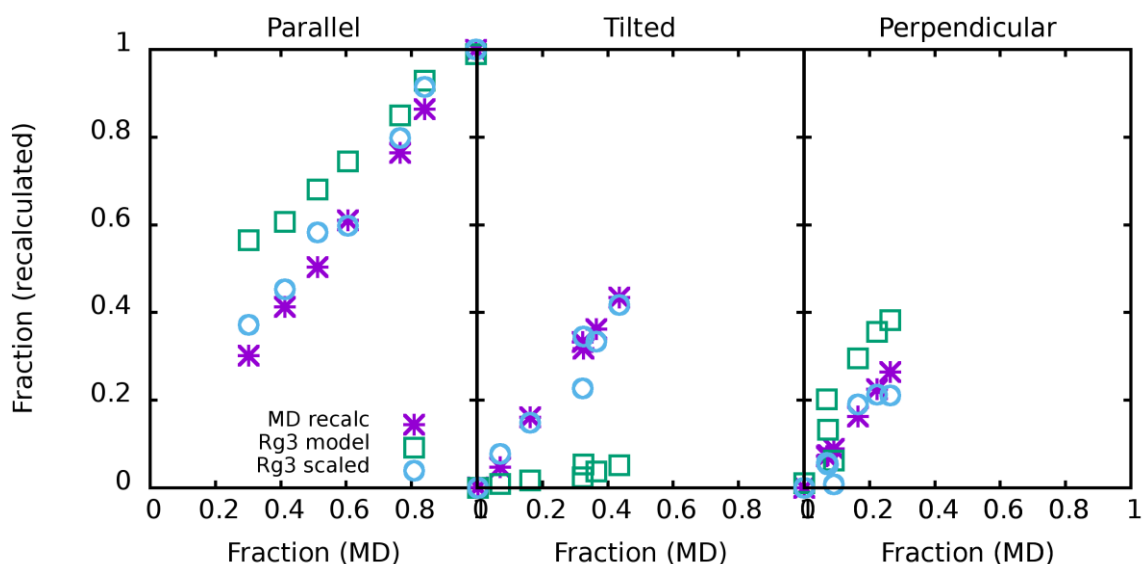


Figure S6: Fraction of parallel (TDM to membrane normal angle θ within $0-30^\circ$), tilted ($30-60^\circ$) and perpendicular ($60-90^\circ$) orientation as monitored in MD simulation (x-axis) and as recalculated from the θ distribution – with $\langle P_2 \rangle$ and $\langle P_4 \rangle$ coming from raw MD ('MD recalc'), from the general Rg3 model and from the Rg3 model with rescaled $\langle P_4 \rangle$ ('Rg3 scaled'). Data from DPPC are omitted here.

Table S3: Experimental data from refs. Ameloot (1984) and Mitchell (1998) and the θ distribution calculated from $\langle P_2 \rangle$ and $\langle P_4 \rangle$ in terms of fraction parallel ('Par'; the angle θ between TDM and membrane normal is found in a range 0-30°), tilted (30-60°) and perpendicular ('Perp'; 60-90°) orientation. The recalculated data (Eq. 13 in the main text) are shown. If initially a $\langle P_4 \rangle$ lower than 0.5 is reported (grey cells), the recalculation cannot be applied any longer and it does not lead to meaningful distribution.

		DMPC					DPPC					DOPC			
	T (°C)	7.7	16.3	24.3	35.4	42.0	22.3	32.4	40.3	45.4	51.8	10	20	30	40
	Phase	S _o	S _o	T _m	L _d	L _d	S _o	S _o	T _m	L _d					
Original	$\langle P_2 \rangle$	0.88	0.86	0.53	0.28	0.23	0.84	0.81	0.44	0.32	0.27	0.27	0.18	0.21	0.22
	$\langle P_4 \rangle$	0.83	0.79	0.52	0.44	0.40	0.75	0.70	0.54	0.54	0.53	0.42	0.39	0.37	0.34
	Par	95%	94%	69%	51%	47%	92%	90%	64%	57%	53%	50%	44%	44%	44%
	Perp	5%	5%	24%	42%	45%	6%	7%	32%	41%	45%	42%	48%	45%	43%
	Tilted	0%	1%	7%	7%	8%	1%	3%	4%	2%	2%	8%	8%	10%	13%
Rescaled	$\langle P_4 \rangle$	0.70	0.62	0.09	-0.07	-0.14	0.55	0.45	0.13	0.13	0.11	-0.11	-0.17	-0.21	-0.26
	Par	95%	92%	47%	24%	17%	90%	94%	45%	39%	35%	21%	13%	11%	8%
	Perp	2%	0%	6%	20%	20%	0%	0%	16%	26%	30%	18%	22%	17%	12%
	Tilted	4%	7%	47%	56%	64%	10%	6%	40%	35%	36%	61%	65%	72%	81%

Convergence issues

Though the position or mean orientation of DPH could have been identified within several tens of ns after DPH permeation into the membrane, the anisotropy decay required several long simulations. Most of the simulations in DOPC fitted into C_∞ in the range of 0.1 – 0.2, with one outlier of 0.4. When we calculated ROTACF for individual 100 ns windows, (Figure S7) we observed that also here was a trend of decreasing of C_∞ . Although we suppose that prolonging the simulation would lead to further C_∞ decrease, it is not clear whether this behaviour is a fluctuation on a very long time scale or a very slow simulation equilibration.

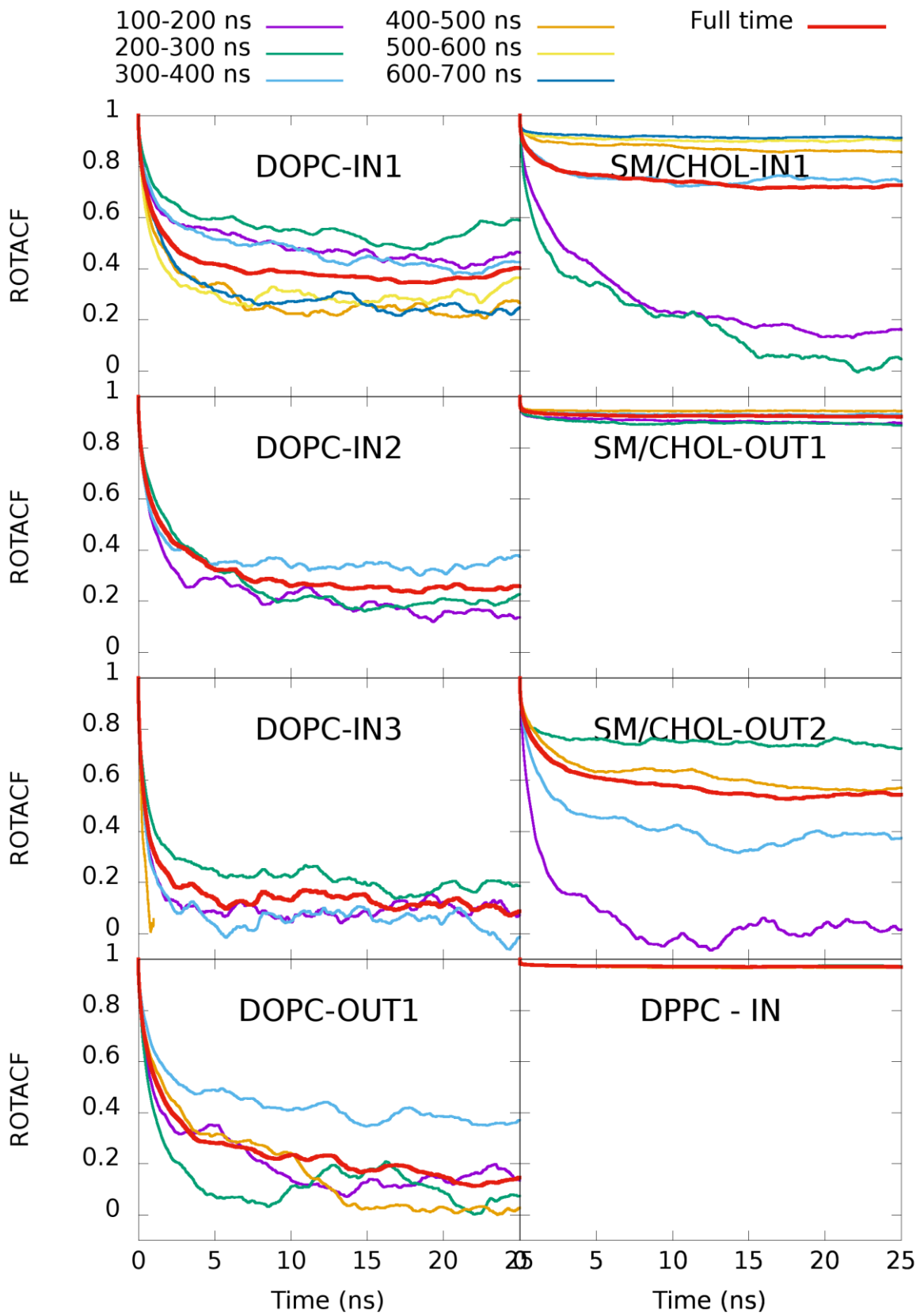


Figure S7: Rotational autocorrelation functions (ROTACF) calculated in individual 100 ns windows and from the whole simulation (after 200 ns of equilibration).

Similar issue was observed for the binary mixture of SM/Chol, which brought further challenges to the analysis of the simulation results. We observed here two kinds of behaviour: Twice (SM/CHOL – IN, OUT2), the DPH was floating along z-axis (Figures S1, S2 and Table S1) and rotating its long axis, in the other simulation (SM/CHOL – OUT1) the DPH adopted a stable location and orientation and did not leave it during the rest of the simulation. Again in SM/CHOL – IN the behaviour of DPH was gradually changing during the simulation and ended in a stable orientation. However, we were aware that as the lipids were randomly distributed in the binary mixture, the membrane was not absolutely homogenous and therefore the local environment of the DPH could differ.

The local environment of the DPH probe

In order to investigate the local environment, the deuterium order parameters $\langle S_{CD} \rangle$ of the closest lipids to DPH were calculated and were compared to each other and to the data extracted from the ROTACFs. The ten closest lipids to the COM of DPH were extracted in each simulation frame and the local $\langle S_{CD} \rangle$ was calculated by averaging over the so created closest lipid tail atoms. We extracted the $\langle S_{CD} \rangle$ of the 10th carbon on lipid acyl tails for each of the simulations and compared them to the calculated C_∞ (Figure S8). In the SM/Chol mixture, we observed that higher local $\langle S_{CD} \rangle$ of lipids correspond to higher C_∞ values, which is indeed another manifestation of the second Legendre polynomial. It exhibits therefore the intrinsic relation between fluorescence anisotropy measurements performed on a probe and a characteristic property of the surrounding phosphatidylcholines.⁴⁵ To our best knowledge however, no such comparison was performed for sphingolipids. Due to differences in the composition of the membrane, in the tilt of lipid tails (in case of DPPC), etc., this comparison cannot be performed here in between different lipid types, but DPH can work as a very local fluidity probe with molecular resolution.

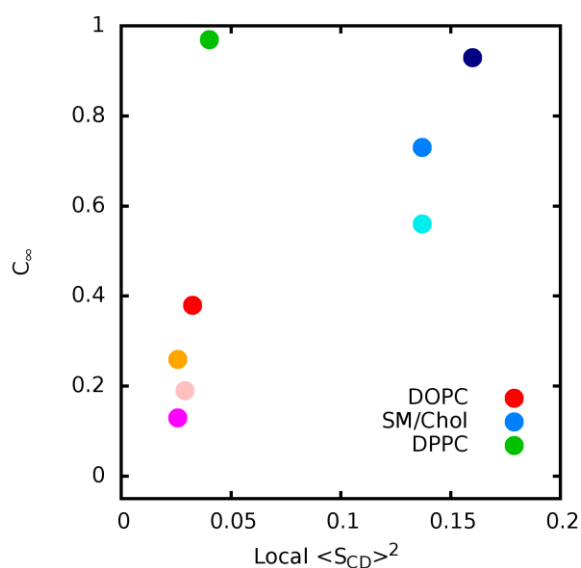


Figure S8: Correlation of the limiting value of ROTACF (C_∞) with the deuterium order parameters $\langle S_{CD} \rangle$ calculated on the 10th carbon of the lipid acyl chains of the ten closest lipids to DPH. The results of the individual simulations for DOPC and SM/Chol are displayed in different shades (red, pink, orange and magenta for DOPC and dark blue, light blue and cyan for SM/Chol). The DPPC $\langle S_{CD} \rangle$ are significantly affected by the tilt of the lipid chains.